

On Prediction of the Strength of the 11-Year Solar Cycle No. 24

V.N. Obridko · B.D. Shelting

Received: 8 June 2007 / Accepted: 5 February 2008 / Published online: 3 March 2008
© Springer Science+Business Media B.V. 2008

Abstract Various forecast techniques have been analyzed with reference to solar activity cycle 24. Three prediction indices have been proposed: the intensity of the polar field, the mean field at the source surface, and a recurrence index of geomagnetic disturbances. As a rule, the forecast based on the polar field and extrapolation of local fields gives a height for cycle 24 that is smaller than that of cycle 23. The use of the recurrence index and the global field value leads us to the conclusion that cycle 24 will be medium high: the same as or somewhat higher than cycle 23.

1. Introduction

The forecast of solar activity for a few years and prediction of characteristics of the following cycles are the oldest problems of solar physics, arising as soon as the solar cycle itself was discovered. Unfortunately, these problems have not yet been solved, probably because, on the one hand, the series of observational data available are not long enough for purely statistical analysis and, on the other, because we do not quite understand the physical nature of the phenomenon. Numerous publications used to appear before each cycle maximum predicting its height in the Wolf number in the range from 60 to 200 (*e.g.*, see reviews in Obridko, 1995; Lantos and Richard, 1998; and Hathaway, Wilson, and Reichmann, 1999). Lately, the unreliability of forecasts has been demonstrated in the current cycle. Kane (2001) has analyzed 20 out of a great number of forecasts of the height of cycle 23 to find out that only 8 of them differed from the true value (claimed to be 122) by less than 20 units.

A full review of the prediction methods available is not the objective of this paper. Some idea can be gathered from Vitinskii (1965), Lantos and Richard (1998), and Hathaway, Wilson, and Reichmann (1999). Here, we shall only mention the main techniques, which are, in fact, not too many. The first method proceeds from the very notion of the solar periodicity. Assuming all cycles to be equal, we can find the length of the cycle and predict its main

V.N. Obridko (✉) · B.D. Shelting
Pushkov Institute of Terrestrial Magnetism, Ionosphere and Radio Wave Propagation, 142190 Troitsk,
Russia
e-mail: obridko@izmiran.ru

dates. Unfortunately, the cycles differ significantly both in duration and in height. Therefore, we have to use spectral analysis (Fourier, spectral-time analysis, or wavelet techniques). Calculations are sometimes made up to the harmonics of very high order. However, reliable observation data are only available for the past 150 years, and so the low-frequency part of the spectrum is calculated with large errors (see McNish and Lincoln, 1949; Calvo, Ceccato, and Piacentini, 1995; Bondar', Rotanova, and Obridko, 1996; and Conway *et al.*, 1998). Various methods have been developed that increase the reliability of forecasts (Chistyakov, 1983; Dmitrieva, Kuzanyan, and Obridko, 2000) and use the internal structure of the cycle (Stewart and Panofsky, 1938; Hathaway, Wilson, and Reichmann, 1999). In fact, all these are the methods of statistical extrapolation.

The recently developed neural modeling used for calculating cyclic curves and forecasting particular events also yields satisfactory results (McPherson, Conway, and Brown, 1995; Fessant, Pierret, and Lantos, 1996; Attia, Abdel-Hamid, and Quassim, 2005; Quassim and Attia, 2007).

Some of these methods have been used to forecast the future cycles. However, the insufficient length of the data series makes the reliability of such forecasts rather poor, though the existence of a longer periodicity approximately equal to 100 years seems quite probable (Kane, 2001, 2002; Khranova, Kononovich, and Krasotkin, 2002)

Now, we shall discuss another group of prediction methods in which the characteristics of the Wolf number cycle are calculated from various heliophysical data. These are the so-called precursor methods. The most popular of them is the method developed in Ohl (1966, 1972) and improved later in Ohl and Ohl (1979). It predicts the height of the following cycle from geomagnetic activity at the descending branch or at the minimum of the previous one. Later, various modifications of this method were proposed (Feynman, 1982; Thompson, 1989, 1993; Obridko, 1995; Lantos and Richard, 1998; Hathaway, Wilson, and Reichmann, 1999). In some cases, this method yields more reliable results than any method of the first group. This should not come as a surprise since the Ohl method proved to be actually the only causal cycle prediction method. In our opinion, the solar cycle is a complicated process of transformation of large-scale fields of one cycle into local fields of the following one. These local fields are what we observe as sunspots. However, the cyclic variation of geomagnetic activity is controlled by the large-scale solar fields (Obridko and Shelting, 1992; Belov, Obridko, and Shelting, 2006).

As a variant of the Ohl method, prediction techniques based on various indices of the large-scale or polar magnetic field have been developed recently. A series of work was performed by the research team headed by V.I. Makarov (see Makarov and Makarova, 1996, and Makarov and Tlatov, 2000). The results were summarized by Tlatov and Makarov (2005). Using $H\alpha$ synoptic magnetic charts and Ca II K-line full-disk spectroheliograms, they developed a set of activity indices of the large-scale background magnetic field. Thus, all global magnetic indices proposed can be used as prediction indices for the activity forecast of local fields for the period of about 5–6 years.

In our opinion, the precursor method is most promising. By the precursor method we mean here the use of data obtained in the declining phase of cycle $N - 1$ to predict the height and timing of the maximum of cycle N . In fact, there is strong evidence that a new cycle is formed on the basis of the previous one. Recall, in particular, the well-known concept of an extended cycle lasting for 17 years (Wilson *et al.*, 1988; Harvey, 1992). Some features of a new cycle (spots, filaments, background fields, coronal holes, and the strength of the polar magnetic field) appear at the descending branch of the old one. Among the forecasts of cycle 21 analyzed at the Working Group A on "Long-term solar activity predictions" of the Meudon Solar-Terrestrial Prediction Workshop in 1984, those obtained by the precursor

method proved to be the most realistic (Brown, 1986). As shown by Schatten and Pesnell (1993), the precursor method is consistent with the implication of dynamo theory that the polar field in the declining phase and at minimum is the seed of future toroidal fields. The panel convened by ten agencies from 9 to 25 September 1996, in Boulder, Colorado, and comprising a dozen scientists from Australia, Germany, the United Kingdom, and the United States (J.A. Joselyn, J. Anderson, H. Coffey, K. Harvey, D. Hathaway, G. Heckman, E. Hildner, W. Mende, K. Schatten, R. Thompson, A.W.P. Thomson, and O.R. White) also gave preference to the precursor technique (Joselyn *et al.*, 1997). When using this method, one should keep in mind that the set of precursors taken to predict the local-field cycle must be based on information on large-scale fields. Note that these data also have certain limitations and do not guarantee success. For example, cycle 23 turned out to be much lower than predicted: with a forecast value of about 160 versus a real value of 120.

In this paper, we are going to calculate the height of cycle 24 from large-scale field data. In Section 2, we shall calculate three types of precursors, and in Section 3 we shall compare our results with the other forecasts available. Note that the unit time for predictors in Sections 2.1 and 2.2 is the Carrington rotation period, and in Section 2.3 it is the Bartels rotation period (27 days). The unit time for relative sunspot numbers is a month or a year. Therefore, the values for a calendar year were calculated for all magnitudes and then an optimal shift was obtained by using the autocorrelation function.

2. Three Precursor Indices Used to Predict the Height of the Next Cycle

2.1. Index of Global Magnetic Field $i(B_r)$

The increasing observational database on global fields has stimulated their systematic analysis, starting from the study of their cyclic behavior. The scenario of the 11-year cycle given in Kuklin, Obridko, and Vitinsky (1990), Obridko and Ermakov (1989), Obridko, Shelting, and Ermakov (1989), Obridko and Shelting (1992), and Ermakov, Obridko, and Shelting (1995a, 1995b) comprise a detailed study of the behavior of local and global magnetic fields. Ermakov, Obridko, and Shelting (1995a, 1995b) introduced the concept of global magnetology of the Sun, in which the description of the cycle is based on global magnetic indices. It proved possible to introduce the notions of the natural length of the cycle as well as normal and abnormal field fluxes. The author proposed a new and (as turned out later) very effective energy index of the global magnetic field, $i(B_r)$, which was determined as the squared radial magnetic field component averaged over the solar surface:

$$i(B_r)|_R = \langle B_r^2 \rangle,$$

where R is the radius of the averaging sphere.

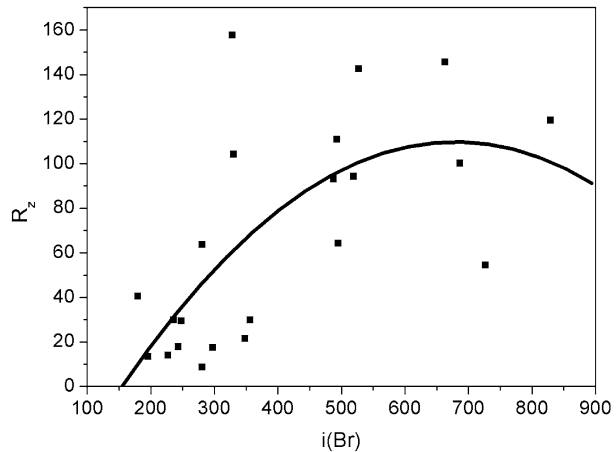
The global field indices introduced in Obridko and Ermakov (1989), Obridko, Shelting, and Ermakov (1989), and Obridko and Shelting (1992) are as follows:

$$i(B_r)|_{R_0} = \sum_{lm} \frac{(l+1+l\zeta^{2l+1})^2}{2l+1} (g_{lm}^2 + h_{lm}^2) \tag{1}$$

in the photosphere and

$$i(B_r)|_{R_s} = \sum_{lm} (2l+1)\zeta^{2l+4} (g_{lm}^2 + h_{lm}^2) \tag{2}$$

Figure 1 The annual mean index $i(B_r)$ compared with the Wolf numbers R_Z with a shift of 9 years.



at the source surface.

These equations were derived for the model of a potential source surface field (*e.g.*, see Hoeksema and Scherrer, 1986). Here g_{lm} and h_{lm} are the Legendre expansion coefficients for the photospheric magnetic field, l and m are, respectively, the spherical harmonic indices, R_0 and R_s are, respectively, the radii of the photosphere and source surface, and ζ is their ratio, assumed to be equal to 0.4. The summation was performed in l and m from 0 to 9.

The coefficients g_{lm} and h_{lm} have been calculated by using the Stanford (WSO) observational data from May 1976 up to the present. The advantage of this index is a relatively weak dependence of its cyclic variation on the assumptions made. In fact, the index $i(B_r)$ calculated for the source surface is the mean squared magnetic field in large-scale coronal holes; therefore, it is closely related to variations of the interplanetary magnetic field.

On the whole, the scenario of the solar cycle is, undoubtedly, the result of interaction of magnetic fields of different scales: local fields with a spatial scale of a few hundredths of the solar radius, large-scale fields of tenths of the radius, and global fields of the order of a solar radius. The contributions from these fields are different and depends on which heliogeophysical process we are considering.

As shown by many authors (*e.g.*, see Obridko and Shelting, 2003, and references therein), the maximum in global fields is observed a few years later than in local ones and 8–9 years prior to the maximum of the following cycle. This gives us the maximum of cycle 24 in 2012. The nine-year shift was confirmed by comparing the annual mean values of the source-surface index $i(B_r)$ and relative sunspot numbers R_Z . The result of the comparison is represented in Figure 1. One can see that the relation between $i(B_r)$ and R_Z is nonlinear and is subject to saturation. The linear approximation gives a correlation with coefficient 0.62 and the quadratic approximation shown in Figure 1 gives a correlation with coefficient 0.69. In 2003, $i(B_r)$ was $785 \mu\text{T}^2$, which yields $R_Z = 128$ in 2012 with the linear approximation and $R_Z = 107$ with the more accurate quadratic approximation.

2.2. Field Intensity at the Pole of the Sun

It is well known that the field intensity at the poles of the Sun reaches a maximum approximately at the minimum of the Wolf numbers, and its height is correlated rather well with the

height of the following cycle. Of course, it seems tempting to use this ratio for prediction. However, one should bear in mind that the very notion of polar field is rather vague.

It is possible to use the directly measured polar magnetic field. The field is, naturally, measured in the photosphere. However, it is not easily done in the immediate proximity of the poles, where the measurements are usually burdened with grave errors. We only measure the longitudinal component of the field, which is virtually horizontal near the poles. And finally, the small- and medium-scale fields cannot be properly filtered out in photospheric measurements (*i.e.*, the directly measured field is not “sufficiently global”).

It is also possible to use the neutral lines of magnetic field inferred from indirect H α data. This method, which is widely used at the Pulkovo Observatory (*e.g.*, see Makarov *et al.*, 2001), is rather simple and reliable, but it does not always give the same results as the previous one.

Having obtained the magnetic field expansion coefficients, one can calculate the polar field at any height (Obridko and Shelting, 1999). This method is applied here. Not only do we use measurements in the immediate proximity of the pole but we also determine the field as though it were constructed from the totality of measurements for a given rotation.

The initial data are magnetic fields calculated from H α synoptic maps by the well-known and repeatedly verified method described next. To study the reversal process, we calculated the global part of such field (the polar field) at two levels: in the photosphere (ph) and at the source surface (ss). All results obtained in this work are based on the polar field data. We can represent the radial solar magnetic field under potential approximation as a function of coordinates (latitude ϑ , longitude φ , and distance r from the center of the Sun) using the method of expansion into harmonics (Hoeksema and Scherrer, 1986; Hoeksema, 1991):

$$B_r = \sum P_n^m(\cos \vartheta)(g_{nm} \cos m\varphi + h_{nm} \sin m\varphi)(n+1)((R_0/R)^{n+1} - n(R/R_s)^{n-1}c_n),$$

where $0 \leq m \leq n < N$ (and we assume in calculations $N = 9$); $c_n = -(R_0/R_s)^{n+2}$, P_n^m are the Legendre polynomials; and g_{nm} and h_{nm} are the spherical harmonic coefficients obtained from the initial data. Considering H α synoptic maps, we took only the sign of the magnetic field: +1 G or -1 G for the positive and negative field, respectively. Knowing the expansion coefficients g_{nm} and h_{nm} , we can reconstruct the synoptic map and analyze the field distribution.

The field is assumed to be potential up to the source surface at $2.5R_0$ where R_0 is the radius of the photosphere. For a detailed description of the method, see Obridko and Shelting (1999). The field at the north pole corresponds to $\cos \vartheta = 1$ and $m = 0$.

Besides using H α data, we also calculated the polar field from direct magnetographic measurements at Mt. Wilson, Kitt Peak, and Stanford. The fields obtained by both methods were compared.

The two lower panels in Figure 2 illustrate the mean polar field in two hemispheres calculated from H α observations in the chromosphere and at the source surface as a function of time in Carrington rotations. The two upper panels show the polar field calculated from magnetographic data. The field measurements at Mt. Wilson and Kitt Peak were taken with magnetographs having different scales than at Stanford, so the h_{nm} and g_{nm} values obtained differed by an order of magnitude. We reduced the Mt. Wilson and Kitt Peak harmonic coefficients to the Stanford system using a simultaneous observation interval (1976–1984) and then formed a single database to calculate the polar field. One can readily see the good agreement among the three upper curves, though they are based on different original data (magnetographic and H α). It is obvious that a complete similarity can hardly be expected, since the magnetographic data give the field intensity at each point, whereas the H α data

Figure 2 The polar field calculated from magnetographic measurements (top two panels) and the mean polar field of both hemispheres in the photosphere and at the source surface as inferred from $H\alpha$ observations (bottom two panels).

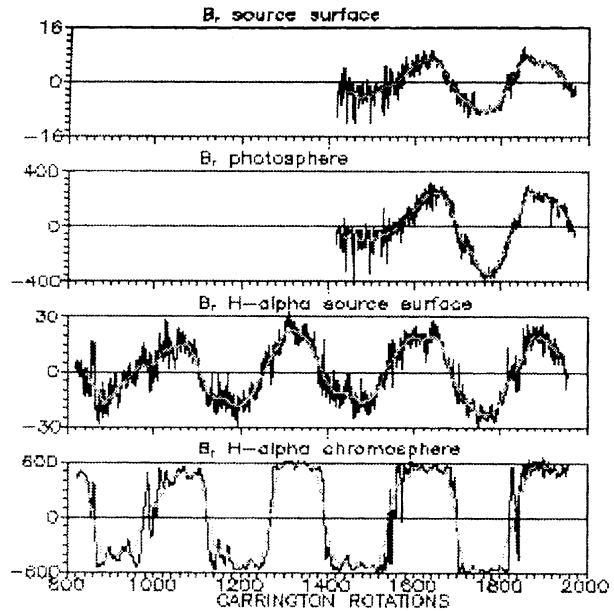
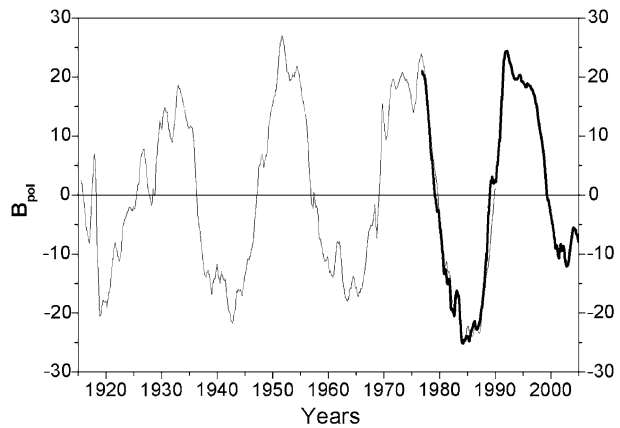


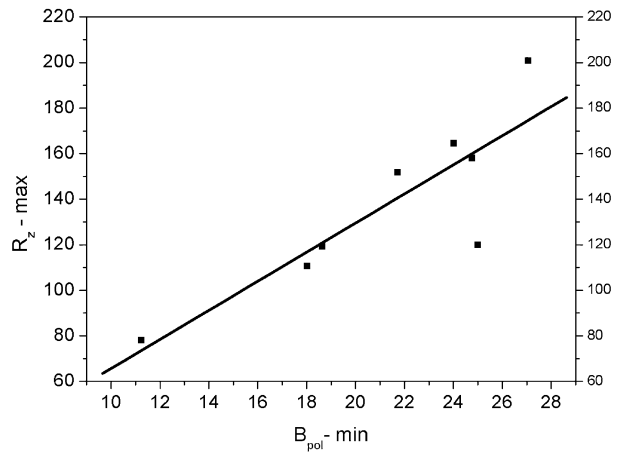
Figure 3 Polar magnetic field calculated from $H\alpha$ data for 1915–1990 (thin curve) and supplemented with calculations based on direct Stanford WSO observations for 1976–2006 (thick curve).



give the areas occupied by the field of one polarity as if all fields in the Sun had the same value and differed only by the sign. However, the agreement is good enough for prediction purposes, and we could combine the polar magnetic field values calculated from $H\alpha$ and magnetographic observations in a single file.

Figure 3 shows the polar magnetic field calculated from $H\alpha$ data for the period 1915–1990. The mean value was calculated (by taking the half-sum of the absolute field values for the north and south hemispheres), and the sign was taken corresponding to the north hemisphere. These data are represented by the thin curve in Figure 3. These data were supplemented with calculations based on direct Stanford WSO observations for 1976–2006 (the thick curve in Figure 3). The scaling factor was calculated for the overlapping interval of 1976–1990 to ensure a single data format. The calculations were made without polar correction. One can see that the data on the overlapping interval agree perfectly well.

Figure 4 Relationship between the polar magnetic field at the global field maximum and the sunspot numbers at the maximum of local fields in the forthcoming cycle.



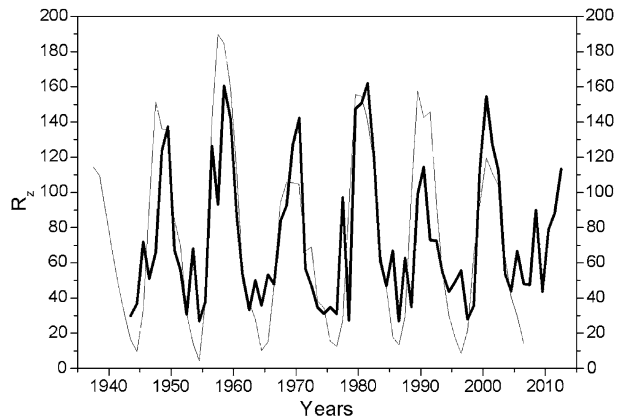
As shown in Makarov *et al.* (2001), the cyclic variations in global fields precede the local-field variations by half a cycle. With this shift taken into account, the correlation between them is about 0.9. Figure 4 represents the dependence between the polar magnetic field at the maximum of the global field cycle and the Wolf numbers at the maximum of the corresponding local field. In Figure 4, the mean effective magnetic field at the pole was calculated as before, by using the data for both hemispheres. The abscissa shows the absolute values of the polar field at the cycle minima, and the ordinate shows the annual mean R_Z values at the maxima of the corresponding cycles. This gives us eight pairs of points for cycles 16–23. One can see that the cross-correlation coefficient is 0.86. It is somewhat decreased owing to an unexpectedly low R_Z at the maximum of cycle 23 mentioned in Section 1.

At the minimum before cycle 24, $B_{\text{pol}} = 12$ (see Figure 3). Therefore, it follows from the regression in Figure 4 that, at the maximum of cycle 24, we should expect $R_Z \approx 80$. It is to be noted that Figures 3 and 4 are based on data from several observatories, which cannot be considered uniform. Therefore, the value of 80 is, probably, somewhat undervalued owing to an unexpectedly low polar field in 2003. However, cycle 23 is not yet over, and the polar field in 2007–2008 may be greater. Then, the predicted value will be changed correspondingly. Note, however, that the forecasts based on the polar field also give low values for the height of cycle 24 (see Section 3).

2.3. Recurrence Index of Geomagnetic Activity

In this section, we use an index based on geomagnetic activity. There are two ideas at the heart of this concept. First, since the pioneering work by Ohl (1966, 1972) and later authors (Ohl and Ohl, 1979; Feynman, 1982; Thompson, 1989, 1993; Obridko, 1995; Lantos and Richard, 1998; Hathaway, Wilson, and Reichmann, 1999), the height of the following cycle has been predicted from the data on geomagnetic activity at the descending branch or at the minimum of the previous one. It is assumed that the local fields and associated sunspots in each cycle have for their basis the large-scale fields in the declining phase of the previous cycle. Besides, it became clear that geomagnetic activity is mainly controlled by large-scale solar fields. A close quantitative relationship between them was revealed by many authors (*e.g.*, see Obridko and Shelting, 1992, and Belov, Obridko, and Shelting, 2006). Thus, in spite of an obvious paradox, variations of the Earth's magnetic

Figure 5 The annual mean Wolf numbers observed (thin curve) and predicted from the recurrence index IR(Ap) (thick curve).



field are precursors of the solar magnetic field variations with a lead time of about 5 years. This relationship is confirmed by rather high correlation coefficients (up to 0.90–0.97) and manifests itself as the so-called prolonged solar cycle.

Note, however, that geomagnetic activity indices reflect both the slow variation determined by large-scale fields (e.g., coronal holes) and storms associated with local fields. Large-scale magnetic fields change slower than local ones. Their structure is more stable and often persists for a few rotations. As a result, geomagnetic disturbances associated with large-scale fields, though smaller in amplitude, can repeat from rotation to rotation. Local fields change faster and produce higher activity usually in a single rotation. Geomagnetic disturbances associated with local fields are generally much stronger and determine the general dynamics of geomagnetic activity.

Therefore, the direct comparison of geomagnetic indices with Wolf numbers shows a high correlation without shift and cannot be used for the forecast of the following cycle. In a paper published in 1982, Feynman pointed out the importance of discriminating two components in the cyclic variation of geophysical parameters: 1. The cyclic component of geomagnetic activity associated with solar activity and 2. The interplanetary component of geomagnetic activity. This idea was used by Hathaway and Wilson (2006) in their recent work dealing with the forecast of cycle 24.

Here, we have divided the components associated with large-scale and local fields using the recurrence index. In doing so, we have considered the main signature of the “interplanetary” component of the Ap index to be its recurrences rather than magnitude (i.e., the fact that the variation curve repeats reliably in the following Bartels rotations). This index was proposed by Sargent (1979) and Levitin *et al.* (1995) and is used with minor modifications in this work.

We took a series of the daily mean Ap values and, shifting it by 27 days, calculated the moving cross-correlation coefficient over the interval of 81 days with a 27-day step. The typical values of the coefficient are 0.2–0.5, but we multiplied these by 500 for convenience of comparison with the Wolf numbers. This is how we found the IR(Ap) index. Then, the IR(aa) index was calculated in the same way from the data. Since they virtually coincide with the correlation coefficient of 0.98, we shall henceforth use IR(Ap).

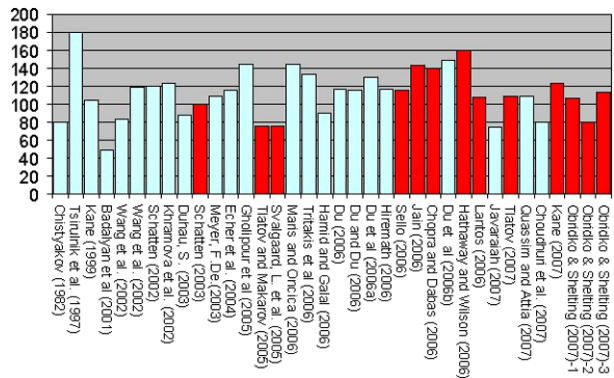
The annual mean values of IR(Ap) and R_Z correlate with a coefficient of 0.77 at a shift of 6 years. The thin curve in Figure 5 shows the measured annual mean R_Z values and the thick curve indicates the values calculated from IR(Ap). Thus, the lower limit of the Wolf number forecast for 2012 is 113.

3. Discussion of Results

Although forecasting the height of the cycle before it begins is often a difficult task with dubious results, there are already numerous publications predicting the parameters of the forthcoming cycle 24. The estimates of the minimum (late 2007 or early 2008) and maximum (the second half of 2010 or the first quarter of 2011) phases seem to be most reliable. As for the height of the cycle, many authors give medium or very low values, just as cycle 23 was mostly expected to be high. This may be due to the very popular idea of a 100-year modulation of solar activity, particularly, as regards the forecasts based directly on the Wolf numbers. Thus, taking into account the secular cycle, Duhau (2003) gives the value 87.5 ± 23.5 , Wang *et al.* (2002) the value 83.2–119.4, and de Meyer (2003) 110 ± 15 . As early as 1983, Chistyakov claimed that cycles 23 and 24 would be low (about 80, with cycle 24 lower than 23). However, a spectral analysis by the global minimum method (Tsilunlik, Kuznetsova, and Oraevsky, 1997) yields a value as high as 180 and the maximum in 2014. Hamid and Galal (2006) and Quassim and Attia (2007) obtained, respectively, values of 91 and 110 based on neural modeling. Maris and Oncica (2006) used the neural network method to obtain a value of 145 and a maximum as early as December 2009. Gholipour *et al.* (2005) obtained the same value of 145 by spectral analysis and fuzzy neural network modeling. Using the maximum entropy method, Kane (1999) isolated the main maxima in the spectrum and predicted the height of cycle 24 to be 105 ± 9 . Echer *et al.* (2004) obtained 115–117 with spectral characteristics. Khramova, Kononovich, and Krasotkin (2002) obtained low values of the forthcoming cycle (123–124) by smoothing over 8 months. Analyzing the number of flares, Maris, Popescu, and Besliu (2004) arrived at the conclusion that cycle 24 had to be low. Javaraiah (2007) obtained the value of 74 from the data on sunspot groups, and Hiremath (2007) predicted 116 using the model of a cycle as a harmonic oscillator. Contradictory results are reported by a number of authors (Du, 2006; Du and Du, 2006; Du, Wang, and He, 2006; Du *et al.*, 2006), who give Wolf numbers at the maximum of cycle 24 equal to 115, 116, 131, and 150.

The precursor models based on the polar field or $H\alpha$ data often yield even lower values of the forthcoming cycle. In Tlatov and Makarov (2005), the forecast with the topological index of the magnetic neutral lines as the precursor gives $R_{Z\text{ MAX}}(24) \approx 75 \pm 10$, and the forecast using the polarity correlation between the background fields in the northern and southern hemispheres yields $R_{Z\text{ MAX}}(24) \approx 70 \pm 10$. Also, from the polarity field data, Schatten (2003) gives a height value of about 100 ± 30 . In his earlier work (Schatten, 2002), he obtained a height for the maximum equal to 120 ± 40 with minimum occurring in April 2011; however, those calculations were made by using both polar and toroidal field data. The analysis of the polar field carried out by Svalgaard, Cliver, and Kamide (2005) suggests that cycle 24 might be the lowest for the past 100 years with a height of 75 ± 8 . Tlatov (2007) studied the relationship between the duration and height of the prolonged solar cycle from $H\alpha$ data and obtained a height value of 100. Including the polar field data into the dynamo model, Choudhuri, Chatterjee, and Jiang (2007) found that cycle 24 would be 35% lower than cycle 23 (*i.e.*, the expected height had to be about 80). In fact, the precursor method was used by Lantos (2006), who considered the skewness of the previous cycles (a classical asymmetry coefficient in statistics) separated into even/odd cycles, and obtained 108. Sello (2003) combined the precursor method with nonlinear extrapolation. Later, in 2006, he revised his calculations to obtain 115 (<http://www.sec.noaa.gov/SolarCycle/SC24>). Our calculations (see Section 2.2) performed with the use of the polar field as the precursor give a low height value. Note that a very low height of cycle 24 (about 50, which seemed then incredible) was obtained by Badalyan, Obridko, and Sykora (2001) from coronal observations.

Figure 6 Summary of different forecasts for the height of cycle 24. The red bars denote the forecast based on precursor data.



Much greater values of the cycle 24 maximum are obtained if the forecast is based on geomagnetic data as the precursor or on dynamo theory. Thus, Jain (2006) obtained 144 using the aa index in the declining phase as the precursor (*i.e.*, a procedure similar to the Ohl method), and Kane (2007) obtained 124 by the Ohl method. Chopra and Dabas (2006) used the monthly mean number of days with $A_p > 25$ and obtained a height of cycle 24 equal to 140. Hathaway and Wilson (2006) give a value of 160 based on geomagnetic activity at the minimum. Dikpati and Gilman (2006) developed a predictive tool based on a Babcock – Leighton-type flux-transport dynamo model of the solar cycle. Calculations by this method give a maximum of cycle 24 equal to 160–180 (*i.e.*, 30–50% higher than the maximum of cycle 23). We have obtained values of 131 with the integral index $i(B_r)$ (see Section 2.1) and 113 with the recurrence index (Section 2.3).

Different forecasts of the height of cycle 24 are summarized in Figure 6. The red bars denote the forecast based on precursor data.

Thus, a large spread of forecasted values is associated not only with the uncertainty of data but also with discrepancies in the long-term variation of the indices used. In particular, the forecast based on polar data is somewhat lower than the forecasts based on other precursors, which give a height of cycle 24 equal to 100–125 units (*i.e.*, the same as or somewhat higher than cycle 23).

Acknowledgements This work was supported by the Russian Foundation for Basic Research (Project No. 05-02-16090).

References

- Attia, A.-F., Abdel-Hamid, R., Quassim, M.: 2005, *Solar Phys.* **227**, 177.
 Badalyan, O.G., Obridko, V.N., Sykora, J.: 2001, *Solar Phys.* **199**, 421.
 Belov, A.V., Obridko, V.N., Shelting, B.D.: 2006, *Geomagn. Aeron.* **4**, 456.
 Bondar', T.N., Rotanova, N.M., Obridko, V.N.: 1996, *Astron. Lett.* **22**, 562.
 Brown, G.M.: 1986, In: Simon, P.A., Heckman, G., Shea, M.A. (eds.) *Solar-Terrestrial Predictions*, NOAA, Boulder, 1.
 Calvo, R.A., Ceccato, H.A., Piacentini, R.D.: 1995, *Astrophys. J.* **444**, 916.
 Chistyakov, V.F.: 1983, *Soln. Dannye* **1**, 97.
 Chopra, P., Dabas, R.S.: 2006, 36th COSPAR Scientific Assembly, Abstract No. 909 (in CDROM).
 Choudhuri, A.R., Chatterjee, P., Jiang, J.: 2007, *Phys. Rev. Lett.* **98**, 131103.
 Conway, A.J., McPherson, K.P., Blacklaw, G., Brown, J.C.: 1998, *J. Geophys. Res.* **103**, 29733.
 de Meyer, F.: 2003, *Solar Phys.* **217**, 349.
 Dikpati, M., Gilman, P.A.: 2006, *Astrophys. J.* **649**, 498.

- Dmitrieva, I.V., Kuzanyan, K.M., Obridko, V.N.: 2000, *Solar Phys.* **195**, 209.
- Du, Z.L.: 2006, *New Astron.* **12**, 29.
- Du, Z.L., Du, S.: 2006, *Solar Phys.* **238**, 431.
- Du, Z.L., Wang, H.N., He, X.T.: 2006, *Chin. J. Astron. Astrophys.* **6**, 489.
- Du, Z.L., Wang, H.N., He, H., Cui, Y.M., Li, R., Zhang, L.Y., He, Y.L.: 2006, 36th COSPAR Scientific Assembly, Abstract No. 473 (in CDROM).
- Duhau, S.: 2003, *Solar Phys.* **213**, 203.
- Echer, E., Rigozo, N.R., Nordemann, D.J.R., Vieira, L.E.A.: 2004, *Ann. Geophys.* **22**, 2239.
- Ermakov, F.A., Obridko, V.N., Shelting, B.D.: 1995a, *Astron. Rep.* **39**, 86.
- Ermakov, F.A., Obridko, V.N., Shelting, B.D.: 1995b, *Astron. Rep.* **39**, 672.
- Fessant, F., Pierret, C., Lantos, P.: 1996, *Solar Phys.* **168**, 423.
- Feynman, J.: 1982, *J. Geophys. Res.* **87**, 6153.
- Gholipour, A., Lucasa, C., Araabia, B.N., Shafiee, M.: 2005, *J. Atmos. Solar-Terr. Phys.* **67**, 595.
- Harvey, K.: 1992, In: Karvey, K.L. (ed.) *The Solar Cycle*, *ASP Conf. Ser.* **27**, ASP, San Francisco, 580.
- Hamid, R.H., Galal, A.A.: 2006, In: Bothmer, V., Hady, A.A. (eds.) *Solar Activity and its Magnetic Origin*, *IAU Symp.* **233**, 413.
- Hiremath, K.M.: 2007, preprint eprint arXiv:0704.1346.
- Hathaway, D.H., Wilson, R.M.: 2006, *Geophys. Res. Lett.* **33**, L18101.
- Hathaway, D.H., Wilson, R.M., Reichmann, E.J.: 1999, *J. Geophys. Res.* **104**, 22375.
- Hoeksema, J.T.: 1991, *The Solar Magnetic Field 1985 through 1990*, World Data Center A for Solar-Terrestrial Physics, Boulder, Colorado.
- Hoeksema, J.T., Scherrer, P.H.: 1986, *The Solar Magnetic Field 1976 through 1985*, Report UAG-94, World Data Center A for Solar-Terrestrial Physics, Boulder, Colorado.
- Joselyn, J.A., Anderson, J.B., Coffey, H., Harvey, K., Hathaway, D., Heckman, G., et al.: 1997, *EOS* **78**, 205.
- Jain, R.: 2006, In: 36th COSPAR Scientific Assembly, Abstract No. 642 (in CDROM).
- Javaraiah, J.: 2007, *Mon. Not. Roy. Astron. Soc.* **377**(1), L34.
- Kane, R.P.: 1999, *Solar Phys.* **189**, 217.
- Kane, R.P.: 2001, *Solar Phys.* **202**, 395.
- Kane, R.P.: 2002, *J. Geophys. Res.* **107**(A7), SSH 3-1.
- Kane, R.P.: 2007, *Solar Phys.* **243**(2), 205.
- Khramova, M., Kononovich, E., Krasotkin, S.: 2002, In: Wilson, A. (ed.) *Solar Variability: from Core to Outer Frontiers*, *The 10th European Solar Physics Meeting*, SP-506 **1**, ESA, Noordwijk, 145.
- Kuklin, G., Obridko, V.N., Vitinsky, Yu.: 1990, In: Thompson, R.J., Cole, D.G., Wilkinson, P.J., Shea, M.A., Smart, D., Heckman, G. (eds.) *Solar Terrestrial Predictions 1*, NOAA, Boulder, 474.
- Lantos, P.: 2006, *Solar Phys.* **236**, 199.
- Lantos, P., Richard, O.: 1998, *Solar Phys.* **182**, 231.
- Levitin, A.E., Obridko, V.N., Val'chuk, T.E., Golyshev, S.A., Dremukhina, L.A.: 1995, *Geomagn. Aeron.* **35**, N2.
- Makarov, V.I., Makarova, V.V.: 1996, *Solar Phys.* **163**, 267.
- Makarov, V.I., Tlatov, A.G.: 2000, *Astron. Rep.* **44**, 759.
- Makarov, V.I., Tlatov, A.G., Callebaut, D.K., Obridko, V.N., Shelting, B.D.: 2001, *Solar Phys.* **198**, 409.
- Maris, G., Oncica, A.: 2006, *Sun Geosph.* **1**, 8.
- Maris, G., Popescu, M.D., Besliu, D.: 2004, In: Stepanov, A.V., Benevolenskaya, E.E., Kosovichev, A.G. (eds.) *Multi-Wavelength Investigations of Solar Activity*, *IAU Symposium* **223**, Cambridge University Press, Cambridge, 127–128.
- McNish, A.G., Lincoln, J.V.: 1949, *EOS* **30**, 673.
- McPherson, K.P., Conway, A.J., Brown, J.C.: 1995, *J. Geophys. Res.* **100**, 21735.
- Obridko, V.N.: 1995, *Solar Phys.* **156**, 179.
- Obridko, V.N., Shelting, B.D.: 1992, *Solar Phys.* **137**, 167.
- Obridko, V.N., Shelting, B.D.: 1999, *Solar Phys.* **184**, 187.
- Obridko, V.N., Shelting, B.D.: 2003, *Astron. Rep.* **47**, 953.
- Obridko, V.N., Ermakov, F.A.: 1989, *Astron. Tsirk.* **1539**, 24.
- Obridko, V.N., Shelting, B.D., Ermakov, F.A.: 1989, *Astron. Tsirk.* **1540**, 23.
- Ohl, A.I.: 1966, *Soln. Dannye* **12**, 84.
- Ohl, A.I.: 1972, *Soln. Dannye* **12**, 102.
- Ohl, A.I., Ohl, G.I.: 1979, In: Donnelly, R.F. (ed.) *Solar-Terrestrial Predictions 2*, NOAA, Boulder, 258.
- Quassim, M.S., Attia, A.A.: 2007, *Solar Phys.* **243**(2), 253.
- Sargent, H.H., III: 1979, In: McCormac, B.M., Seliga, T.A. (eds.) *Solar-Terrestrial Influences on Weather and Climate*, Reidel, Dordrecht, 101.
- Schatten, K.: 2002, *J. Geophys. Res.* **107**(A11), SSH 15-1.
- Schatten, K.: 2003, *Adv. Space Res.* **32**(4), 451.

- Schatten, K., Pesnell, W.D.: 1993, *Geophys. Res. Lett.* **20**, 2275.
- Sello, S.: 2003, *Astron. Astrophys.* **410**, 691.
- Stewart, J.Q., Panofsky, H.A.A.: 1938, *Astrophys. J.* **88**, 385.
- Svalgaard, L., Cliver, E.W., Kamide, Y.: 2005, *Geophys. Res. Lett.* **32**, L01104.
- Thompson, R.J.: 1989, In: Thompson, R.J., Cole, D.G., Wilkinson, P.J., Shea, M.A., Smart, D., Heckman, G. (eds.) *Solar-Terrestrial Predictions 1*, NOAA, Boulder, 598.
- Thompson, R.J.: 1993, *Solar Phys.* **148**, 383.
- Tsirulnik, L.B., Kuznetsova, T.V., Oraevsky, V.N.: 1997, *Adv. Space Res.* **20**, 2369.
- Tlatov, A.G.: 2007, preprint eprint arXiv:astro-ph/0703681.
- Tlatov, A.G., Makarov, V.I.: 2005, In: Sankarasubramanian, K., Penn, M., Pevtsov, A. (eds.) *Large-Scale Structures and Their Role in Solar Activity*, *ASP Conf. Ser.* **346**, ASP, San Francisco, 415.
- Tritakis, V., Mavromichalaki, H., Giouvanellis, G.: 2006, In: Solomos, N. (ed.) *Recent Advances in Astronomy and Astrophysics: 7th International Conference of the Hellenic Astronomical Society*, *AIP Conf. Proc.* **848**, AIP, Melville, 154.
- Vitinskii, Yu.I.: 1965, *Solar Activity Forecasting*, *NASA TTF-289*, 225.
- Wang, J.L., Gong, J.C., Liu, S.Q., Le, G.M., Sun, J.L.: 2002, *Chin. J. Astron. Astrophys.* **2**, 557.
- Wilson, P.R., Altrrock, R.C., Harvey, K.L., Martin, S.F., Snodgrass, H.B.: 1988, *Nature* **333**, 748.